



Unconventional superconductivity in a two-dimensional repulsive gas of fermions with spin–orbit coupling



Luyang Wang*, Oskar Vafek

National High Magnetic Field Laboratory and Department of Physics, Florida State University, Tallahassee, FL 32306, USA

ARTICLE INFO

Article history:

Received 10 September 2013

Accepted 15 October 2013

Available online 22 October 2013

Keywords:

Spin–orbit coupling

Time-reversal symmetry breaking

Topological superconductivity

ABSTRACT

We investigate the superconducting instability of a two-dimensional repulsive Fermi gas with Rashba spin–orbit coupling α_R . Using renormalization group approach, we find the superconducting transition temperature as a function of the dimensionless ratio $\Theta = \frac{1}{2}m\alpha_R^2/E_F$ where $E_F = 0$ when the smaller Fermi surface shrinks to a (Dirac) point. The general trend is that superconductivity is enhanced as Θ increases, but in an intermediate regime $\Theta \sim 0.1$, a dome-like behavior appears. At a very small value of Θ , the angular momentum channel j_z in which superconductivity occurs is quite high. With increasing Θ , j_z decreases with a step of 2 down to $j_z = 6$, after which we find the sequence $j_z = 6, 4, 6, 2$, the last value of which continues to $\Theta \rightarrow \infty$. In an extended range of Θ , the superconducting gap predominantly resides on the large Fermi surface, while Josephson coupling induces a much smaller gap on the small Fermi surface. Below the superconducting transition temperature, we apply mean field theory to derive the self-consistent equations and find the condensation energies. The state with the lowest condensation energy is an unconventional superconducting state which breaks time-reversal symmetry, and in which singlet and triplet pairings are mixed. In general, these states are topologically nontrivial, and the Chern number of the state with total angular momentum j_z is $C = 2j_z$.

© 2013 Elsevier B.V. All rights reserved.

1. Introduction

Unconventional superconductivity arising from purely repulsive fermion interactions was first studied by Kohn and Luttinger [1]. Although the bare interaction is repulsive, screening effects can give rise to attraction between fermions. In three dimensions, *p*-wave superconductivity is found at second order in the interaction [1], while for a strictly parabolic dispersion in two dimensions (2D), it is known that repulsive interaction does not induce superconductivity to second order in the interaction, and one has to go to third order for the occurrence of superconductivity [2]. Since spin–orbit coupling plays an important role in many condensed matter systems, such as topological insulators, noncentrosymmetric systems, and some oxide interfaces, it is natural to ask: what is the role of spin–orbit coupling in this process? Does it enhance superconductivity? And what is the nature of the superconducting state? In this paper, we investigate the unconventional superconductivity in two-dimensional (2D) repulsive Fermi gas with Rashba spin–orbit coupling. (The superconductivity of Rashba model with attractive interaction has been addressed in Ref. [3–5].)

In an earlier paper [6], we have reported some main results of this work. In this paper, we include the details of the calculations.

In addition, we clarify the pairing symmetry and topological properties of the unconventional superconducting states we found.

In Rashba model, the strength of the spin–orbit coupling is characterized by the parameter α_R , which is tunable by the application of an external electric field perpendicular to the 2D system. We treat the Rashba spin–orbit coupling α_R nonperturbatively, so we can analyze the relative values of the mean-field transition temperature T_c for an arbitrary value of the dimensionless ratio $\Theta = \frac{1}{2}m\alpha_R^2/E_F$, where m is the (bare) fermion mass and E_F is the Fermi energy, measured from the Dirac point. In the strictest sense, in 2D Kosterlitz-Thouless theory should be used to treat the phase transition, and the transition temperature $T_{KT} < T_c$. However, since we are working in the weak coupling limit, the pairing energy scale is much smaller than the zero temperature phase stiffness energy and $1 - T_{KT}/T_c \sim T_c/E_F \ll 1$, justifying the approach presented here.

Our study is formulated within the renormalization group (RG) approach [7]. We integrate out high energy modes, and derive effective interactions for low energy modes. We perturbatively calculate the renormalization of the interactions, and derive the RG flow equations which describe how the interactions evolve with lowering the energy. The effective interactions, as well as the RG equations, can be decoupled in angular momentum channels. Although singlet and triplet pairs are mixed by spin–orbit coupling [4], since the Hamiltonian commutes with the *z*-component of the total angular momentum, $J_z = L_z + S_z$, we can label the pair states according to j_z , the eigenvalue of J_z . The decoupled effective inter-

* Corresponding author. Tel.: +1 8502731832.
E-mail address: lw07c@my.fsu.edu (L. Wang).

actions in each channel follow the same RG equation, but have different initial values. In some channels, they diverge at some energy scale as the RG flow runs. Among all the channels, the highest energy scale at which the divergence occurs is identified with the superconducting transition temperature.

The Fermi surface splits into two due to spin–orbit coupling, a large one and a small one, with helicity $\lambda = +1$ and -1 , respectively. We find that the superconducting gap residing on the large Fermi surface always dominates, while momentum space Josephson coupling induces superconductivity on the small Fermi surface. The superconductivity is enhanced by spin–orbit coupling, since now it appears at second order of the repulsive interaction instead of third order. With Θ increasing from small values to infinity, the angular momentum channel j_z in which Cooper pairs condense decreases as an arithmetic sequence with step 2, with an exception in the intermediate range of Θ (see Fig. 6). In the limit of large Θ , we find $j_z = 2$. Our results can also be derived diagrammatically by summing the leading logarithms to all orders in perturbation theory, as has been done traditionally in treating Kohn–Luttinger effect [8,9]. Also, our approach is similar to that of Ref. [10] (see also [11]), which implements a two-step RG by first eliminating high energy modes down to an artificial cutoff and then running the RG flow from the cutoff. However, our single step RG is more economical.

In the superconducting state, mean field theory is applied to find the self-consistent equations and the condensation energies. There are two solutions to the self-consistent equations, one fully gaps the Fermi surfaces and breaks time reversal symmetry (TRS), and the other has gap nodes and does not break TRS. The former has a lower condensation energy, hence is the physical state. In this state, only one of the two $\pm j_z$ pairing components is finite, and singlet and triplet pairings are mixed. For example, $j_z = 2$ state is a mixture of $d_{x^2-y^2} + id_{xy}$ singlets, $p_x + ip_y$ spin-up triplets and $f_{x^3-3xy^2} + if_{3x^2y-y^3}$ spin-down triplets. These TRS breaking states are topologically nontrivial, with the Chern number $C = 2j_z$.

It is convenient to define a three-component vector \vec{D}_λ in such a way that the gap function on helicity- λ Fermi surface is $(\vec{D}_\lambda \cdot \vec{\Sigma})(i\sigma_y)$, where $\vec{\Sigma} = (\sigma_x, \sigma_y, \mathbb{1})$. For a general noncentrosymmetric superconductor, the gap function is usually defined as $(\psi\mathbb{1} + \vec{d} \cdot \vec{\sigma})(i\sigma_y)$ where ψ is the order parameter for spin-singlet pairing while \vec{d} is that for spin-triplet pairing. In our case, the z -component of the \vec{d} -vector is zero since all the triplets are polarized. So we combine the x - and y -component of \vec{d} with ψ to form the new vector \vec{D}_λ . In this way the gap function can be represented by \vec{D}_λ , which can be viewed graphically. We find

$$\vec{D}_\lambda = \Delta_\lambda i\lambda e^{i j_z \theta_{\mathbf{k}}} (\sin \theta_{\mathbf{k}}, -\cos \theta_{\mathbf{k}}, -\lambda), \quad (1)$$

where Δ_λ is the pairing amplitude on the helicity- λ Fermi surface. We plot \vec{D}_\pm (without the phase factor) around the two gapped Fermi surfaces schematically in Fig. 1.

This paper is organized as follows. In Section 2, we set up the Hamiltonian and solve the eigenenergies and eigenstates for the noninteracting Hamiltonian. In Section 3, we formulate the problem using path integrals, and perturbatively expand the action to second order. Two diagrams, the particle–particle bubble and particle–hole bubble, contribute to the renormalization of the interaction. In Section 4, we explicitly calculate the particle–hole bubble, which will show up in our final expression for the superconducting transition temperature. In Section 5, the higher order expansion is calculated, to serve as the RG flow. In Section 6, RG approach is applied, and the decoupled flow equations are found and solved in each angular momentum channel. In Section 7, the effective couplings and superconducting transition temperature T_c are computed. The symmetry and topological properties of the unconventional superconducting

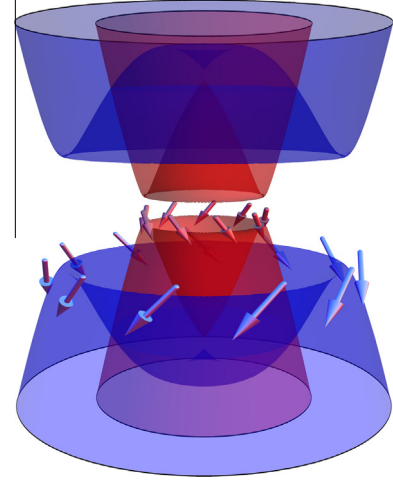


Fig. 1. A schematic plot of \vec{D}_λ (without the phase factor) around the two gapped Fermi surfaces.

states are illustrated in Section 8. We summarize the paper in Section 9. The mean field theory below T_c , including the Ginzburg–Landau theory, is derived in Appendix A.

2. Hamiltonian

We start from the single particle Hamiltonian of a two-dimensional Fermi gas with spin–orbit coupling,

$$H = H_0 + H_{SO} + H_{int}, \quad (2)$$

where the free electron term is

$$H_0 = \frac{\mathbf{k}^2}{2m}, \quad (3)$$

the spin–orbit coupling term is

$$H_{SO} = \alpha_R (\boldsymbol{\sigma} \times \mathbf{k}) \cdot \hat{\mathbf{n}} = \alpha_R (\sigma_x k_y - \sigma_y k_x) = \alpha_R k \begin{pmatrix} 0 & ie^{-i\theta_{\mathbf{k}}} \\ -ie^{i\theta_{\mathbf{k}}} & 0 \end{pmatrix}, \quad (4)$$

where σ 's are Pauli matrices, and the interacting term H_{int} is dealt with later. Here $\theta_{\mathbf{k}}$ is the angle between \mathbf{k} and k_x -axis. The eigenenergies of the noninteracting Hamiltonian are

$$\epsilon_{\mathbf{k}\lambda} = \frac{k^2}{2m} - \lambda \alpha_R k = \frac{(k - \lambda k_R)^2}{2m} - \frac{k_R^2}{2m}, \quad (5)$$

and the corresponding eigenstates are

$$\eta_{\mathbf{k}\lambda} = \frac{1}{\sqrt{2}} \begin{pmatrix} 1 \\ i\lambda e^{i\theta_{\mathbf{k}}} \end{pmatrix}, \quad (6)$$

where $k_R = m\alpha_R$, $\lambda = \pm 1$ and $k_\lambda = k_F + \lambda k_R$ with $k_F = \sqrt{2mE_F + k_R^2} = \sqrt{k_F^{(0)2} + k_R^2}$. The Fermi surface is split into two Fermi surfaces by spin–orbit coupling, with different helicities. In second quantization form,

$$H_0 = \sum_{\mathbf{k}\lambda} \frac{k^2}{2m} c_{\mathbf{k}\lambda}^\dagger c_{\mathbf{k}\lambda}, \quad (7)$$

$$H_{SO} = \alpha_R \sum_{\mathbf{k}\alpha\beta} c_{\mathbf{k}\alpha}^\dagger [(\boldsymbol{\sigma}_{\alpha\beta} \times \mathbf{k}) \cdot \hat{\mathbf{n}}] c_{\mathbf{k}\beta}, \quad (8)$$

where $c_{\mathbf{k}\lambda}^\dagger$ and $c_{\mathbf{k}\lambda}$ creates and annihilates fermions with spin $\lambda = \uparrow$ or \downarrow and momentum \mathbf{k} , respectively. Diagonalized in the helicity basis, the kinetic Hamiltonian becomes

Download English Version:

<https://daneshyari.com/en/article/8164633>

Download Persian Version:

<https://daneshyari.com/article/8164633>

[Daneshyari.com](https://daneshyari.com)